Stitching-Error Reduction in Gratings by Shot-Shifted Electron-Beam Lithography

David J. Dougherty, Richard E. Muller, Paul D. Maker, and Siamak Forouhar

***Abstract*—Calculations of the grating spatial-frequency spectrum and the filtering properties of multiple-pass electron-beam writing demonstrate a tradeoff between stitching-error suppression and minimum pitch separation. High-resolution measurements of optical-diffraction patterns show a 25-dB reduction in stitching-error side modes.**

***Index Terms*—Diffraction, electron-beam lithography, gratings, integrated optics, semiconductor lasers.**

I. Introduction

GRATINGS are a fundamental optical element for wavelength control in photonic devices. Electron-beam lithography offers the submicron resolution required to form first-order gratings in the visible- and near-infrared, as well as the flexibility to implement multiple pitches on the same chip, and longitudinal variations such as chirp and phase shifts. Because of the finite sweep range of the electron beam deflector system, patterns must be stitched together by moving the sample on a mechanical stage. Miscalibration between the beam deflectors and stage travel causes interruptions in the pattern at the field boundaries. This mismatch can occur during a run for a number of reasons, including tilt of the sample or thermal drift. Often, stitching error varies from run to run, making its source difficult to determine. Because its effects are often not observed until device testing, a reliable method to reduce stitching error is of interest.

Stitching error can have both random and systematic components. The distribution of random errors for the JEOL JBX-5D2 machine (JEOL USA, Peabody, MA 01960) at the Jet Propulsion Laboratory (JPL), California Institute of Technology, Pasadena, CA, is quoted by the manufacturer to have a 90-Å three-sigma width. Kjellberg *et al.* have made a detailed study of the impact of random stitching errors of this order of magnitude on the single-mode yield and performance of semiconductor distributed feedback (DFB) lasers [1]. They concluded that random errors on this scale do not seriously affect laser performance. Systematic errors can have a much greater impact on grating structures because they generate scattered waves, which add coherently. Systematic stitching error in DFB lasers can cause lasing on side modes separated from the main stopband by 3 to 5 nm, depending on field size. Implementation of $\lambda/4$ phase-shifted and corrugation pitch modulated (CPM) lasers [2] is not possible in the presence of these uncontrolled phase interruptions. The exact relationship between the side mode ratio (SMR) of the grating spatial frequency and the SMR observed in optical emission is a complicated function of the gain spectrum, its saturation properties, and mode competition effects, as well as the laser structure and cavity design. However, simple multiple-pass writing techniques can reduce the grating stitching-error side modes by at least 25 dB, as will be shown below. Reductions of this order of magnitude completely eliminate unwanted modes in the standard 500-long ridge waveguide DFB lasers fabricated at JPL. The analysis presented in this paper is intended to guide design of multipass schemes, which can be tailored to suit different applications as both active and passive devices.

One way to overcome stitching error is to operate in a mode with a field size large enough to accommodate an entire device. Because the beam position is digitally controlled, this places a limitation on available pitch sizes. The pattern can be rescaled with analog controls, but this is not desirable for applications such as repeatable high-yield fabrication of DFB lasers matched to specific molecular-absorption lines. Careful alignment using deflection-amplitude calibration marks have been used to reduce error to less than 5 nm [3]. This requires extra processing steps, however.

Multiple-write techniques have been used previously to reduce stitching error. Muroya *et al.* [4] used precisely weighted doses at different positions to shape the individual grating-tooth profiles to achieve positioning below the stage motion resolution limit. Albert *et al.* used multiple scans with different field sizes for long-phase mask gratings [5]. Tiberio *et al.* [6] used an interesting voting technique for stage-position averaging that allows for continuous writing in a single scan across the wafer. Their basic multiple-write scheme, denoted as shot shifting for brevity in the rest of this paper, is depicted in Fig. 1. The top drawing shows the standard writing process where a full dose is written in each field. The lower drawing illustrates the case of four-level shot-shifting, writing at one fourth of the dose and moving the stage every one fourth of the field. Intuitively, aside from the initial and final ramp-up and ramp-down fields, the effect of the multiple exposures is to average the stitching error present at the end of the field over each tooth of the grating. Appropriate field patterns can be inserted into the program to allow for abrupt terminations of the grating if desired.

However, this explanation does not completely account for the spectral properties, the number of passes required, or the effectiveness of this process. In this work, we use a simple linear theory [7] that describes the action of multiple writing passes as a filter on the grating spatial frequency spectrum, to examine the tradeoffs in designing optical gratings. In addition, optical

Manuscript received July 5, 2000; revised June 5, 2001.

D. J. Dougherty is with Scion Photonics, Milpitas, CA 95035 USA (e-mail: david.dougherty@scionphotonics.com).

R. E. Muller, P. D. Maker, and S. Forouhar are with the Microdevices Laboratory, Jet Propulsion Laboratory (JPL), California Institute of Technology, Pasadena, CA 91109 USA.

Publisher Item Identifier S 0733-8724(01)08789-8.

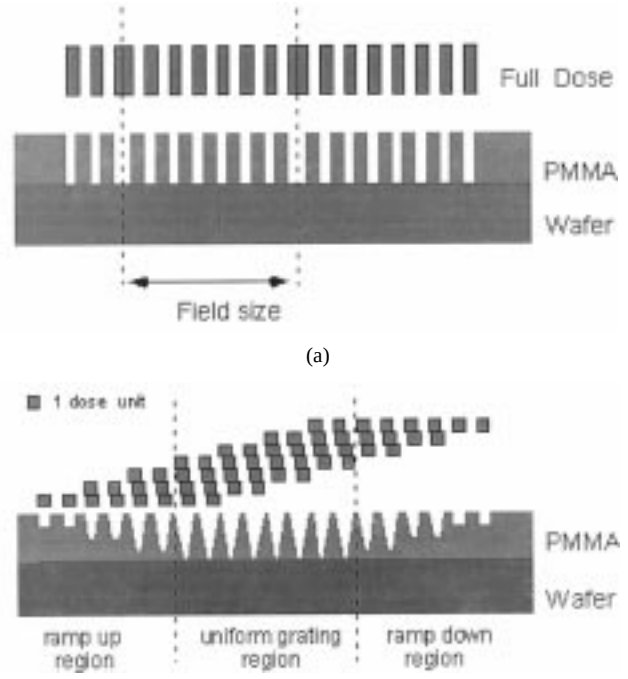

Fig. 1. (a) Standard e-beam process uses a full dose across one field, then moves stage to next field. (b) Shot-shift process for $M = 4$ levels writes at one fourth of the dose and moves stage every one fourth of a field.

diffraction measurements of the side band suppression are described that quantify the achievable nulling effect.

II. Theory

A. Stitching-Error Spectrum

The effect of stitching error on the grating frequency spectrum is considered first. We are concerned with first-order diffraction, so only the fundamental harmonic of the assumed rectangular grating need be considered. The grating is composed of fields of length L. The period is T with corresponding wave vector K_T, and there are an integer number of periods, N in a field; thus, $L = NT$. This field pattern is repeated at intervals of $L + \Delta x$ where Δx is the stitching error. The spatial frequency spectrum is given by an expression involving two factors

$$G(k) = G_L(k)S(k) = \left[\frac{\sin(k-K_T)L/2}{(k-K_T)L/2} - \frac{\sin(k+K_T)L/2}{(k+K_T)L/2}\right] \cdot \sum_{n=0}^{\infty} \delta\left(k - \frac{2\pi n}{L+\Delta x}\right). \quad (1)$$

The first factor is the spectrum of a single field. The second factor describes the effect of tiling the grating as sampling of the single-field spectrum. When $\Delta x = 0$, the delta comb samples at the peak of the sinc function because $K_T = (2\pi N/L)$. The rest of the delta functions fall on the zeros of the sinc function and the spectrum corresponds to that of an infinite sinusoid. When $\Delta x \neq 0$, the δ functions move off the zeros, giving rise to spectral sidebands roughly separated at intervals of the field-wave vector $2\pi/L$. Assuming $\Delta x \ll L$ and $N \gg 1$, the size of the shift in wave vector of the modes near $k = K_T$ is given approximately by

$$\Delta k = \frac{2\pi}{L}\frac{\Delta x}{T}. \quad (2)$$

When $\Delta x = T/2$, a $\lambda/4$ phase shift, the peaks shift to give two equal modes symmetric about K_T. For $\Delta x = T$, the peaks shift so that there is again one central mode, but the side modes now do not fall exactly on the zeros of the sinc functions; thus, there remains a small set of stitching-error sidebands. In a scalar diffraction model (at small impressed phase shift), the diffracted optical power is given by $|G(k)|^2$, which implies that the observed stitching side modes go as $(\Delta x/T)^2$. Fig. 2 shows the relationship between these components for the case of $T = 1$ unit and $N = 150$ periods per field with k measured in units of $2\pi/L$. The dashed curve is the sinc-function spectrum of a single field, the dashed arrow represents the single delta function for the case of $\Delta x = 0$, and the solid arrows show the modes for $\Delta x = T/4$, a $\lambda/8$ shift.

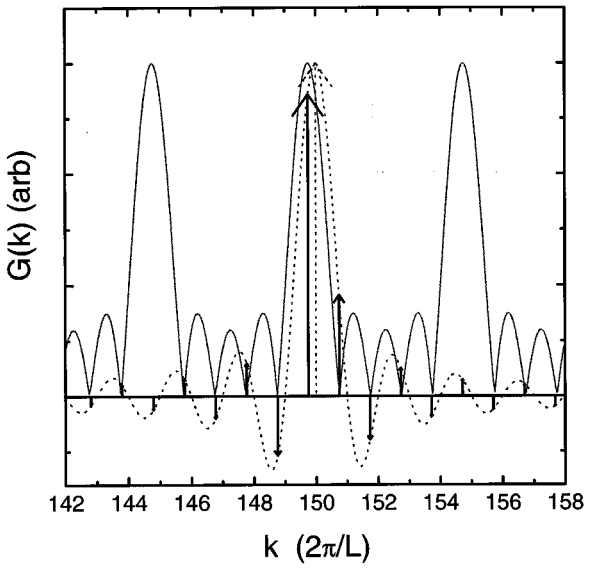

Fig. 2. Effect of stitching error on the grating spatial frequency spectrum. Dashed line: Sinc line shape of a single field of $N = 150$ periods ($T = 1$, $L = NT$). Dotted arrow: Single component selected when stitching is perfect. Solid arrows: Sideband frequency components arising for the case of $1/4$ period $(T/4)$ stitching error. Solid line: absolute value of the shot-shift filtering function for $M = 5$ showing nulling of the nearest sidebands.

The results, so far, are for the case of systematic stitching errors. For random stitching errors, the averaged spatial-frequency spectrum is of interest. Assuming Gaussian-distributed errors, and using standard properties of Fourier transforms, the grating spatial-frequency spectrum can be expressed as

$$G_R(k) = G_L(k) \sum_{n=-\infty}^{\infty} \exp\left(-\frac{L^2}{2\sigma_x^2 k^2}\left(k - \frac{2\pi m}{L}\right)^2\right) \quad (3)$$

where σ_x is the variance of the stitching error. Random errors replace the delta sampling comb of (1) with a train of Gaussian pulses in the spatial frequency domain. The pulsewidth of this sampling function depends slowly on k

$$\sigma_k = \sigma_x \frac{k}{L} \quad (4)$$

indicating that higher order grating harmonics will suffer more from random stitching-error broadening. For the first-order diffraction considered here, $k = K_T$ and $m = N$. Thus, near the central peak, the spectral widths of the diffracted modes are approximately

$$\sigma_N = \left(\frac{2\pi}{L}\right)\frac{\sigma_x}{T}. \tag{5}$$

B. Shot-Shift Spectrum

Now that the grating spatial frequency spectra have been calculated, the effect of the shot shifting can be addressed. In the shot-shift process, the grating with stitch errors is written M times at $1/M$ dose and shifted by moving the stage a distance $1/M$ of one field. In the spatial domain, the resulting grating $g_{\rm SS}$ is given by

$$g_{\rm SS}(x) = \frac{1}{M}\sum_{m=1}^{M} g\left(x - \frac{L+\Delta x}{M}\right). \tag{6}$$

Note that stitching error Δx is included because the shifts are introduced by the stage motion. These spatial delays give rise to filtering in the frequency domain. The spectrum of the shot-shifted grating is given by

$$\begin{aligned} G_{\rm SS}(k) &= F_M(k)G(k) \\ &= \frac{1}{M}\exp\left(ik\frac{L+\Delta x}{2}\left(1-\frac{1}{2M}\right)\right) \\ &\quad\cdot\frac{\sin\left(k\frac{L+\Delta x}{2}\right)}{\sin\left(k\frac{L+\Delta x}{2M}\right)}G(k). \end{aligned} \tag{7}$$

This filtering function F_M has several important properties. First, it possesses a maximum at the main peak of $G(k), k = K_T + \Delta k$, provided N/M is an integer; otherwise, the central peak will be nulled. Second, it has zeros at most multiples of $2\pi/(L + \Delta x)$, the exact positions of the unwanted side modes in $G(k)$. Last, F_M is periodic with period $2\pi M/(L + \Delta x)$. Thus, in this linear approximation, shot shifting uses the stage-motion error to null the nearest $M - 1$ stitching-error sidebands, but leaves the Mth one unaffected. This is illustrated in the solid curve of Fig. 2, which plots the absolute value of $F_M(k)$ for $M = 5$ and the same stitching error as above. M can be chosen large enough to push the nearest surviving stitch-error component out to a distance where it is sufficiently small. As will be discussed below, M should not be chosen too large because it restricts the minimum accessible pitch separation.

The Δx that appears in (6) is the mean-value or systematic part of the stitching error. The random errors can be associated with the M instances of the random process $g(x)$, whereas the shot-shift filter can be assumed to be perfect. Thus, if only random errors are present, the filter function $F_M(k)$ with $\Delta x = 0$ applied to the random stitching-error spectrum of (3) will give the final shot-shifted grating spectrum. One result of this calculation is that shot shifting will not help narrow spectral broadening of the main diffracted peak caused by random stitching error; it only helps suppress sideband spectral components.

III. Diffraction Measurements

The grating functions calculated above really represent the distribution of current dose given to the resist layer on the sample. The development process is designed to be a highly nonlinear function of the current dose for maximum contrast. Thus, the linear theory given above is only approximate. The prediction of exact nulling of the stitching-error components is especially suspect, and experiments must be performed to determine the level of suppression that can be achieved in practice.

To observe the stitching-error suppression, optical-diffraction measurements were performed using an HeCd laser and a high-resolution (0.0001°-encoder count) rotation stage. Adjustable slits were used on the input and output along with 100-mm collimating lenses. The spot on the grating measured 1 cm wide by 1 mm high, and the highest resolution obtained for specular reflection was 2 mdeg. The slits were opened in the actual experiments in order to get enough signal from the ultraviolet photomultiplier tube, resulting in a 11-mdeg full-width at half maximum (FWHM) resolution. The gratings were written in polymethylmethacrylate on InP substrates using 50-keV and 200-pA beam current in the fifth lens. Other parameters include a line dose of 4.5 nC/cm, a clock rate of 2 MHz, and a 5-nm step increment. The base grating pattern was 150 periods of 300-nm pitch lines, giving a field size of 45 μm. Stitching error could be introduced either directly in software by adjusting the stage travel commands or by changing a global system parameter equivalent to changing the sample height. This introduces errors because the e-beam travel is calculated from the angle induced by the beam-deflector plates and the distance to the sample.

Fig. 3 shows angular spectra for the -1 order of four gratings with different shot-shift patterns, and intentionally built-in stitch errors of approximately 26 nm achieved by offsetting the sample height parameter. The top trace was not shot shifted, and sidebands beyond the thirtieth order can be measured. The 0.255°-spacing corresponds to the 45-μm field k-vector. This error is much larger than the inherent error of our machine, but it allows us to measure the effectiveness of the shot-shift filtering by looking at changes in the main mode to SMR. Typical gratings from our machine without shot-shifting have an SMR of -30 dB. These side modes are suppressed below the skirt of the main mode when shot shifting is used. The lower three traces have the same built-in stitching error, but use shot shifting with $M = 2, 3$, and 5. In each case, only sideband orders at integral multiple of $2\pi M/L$ are unaffected, as predicted by (7). The dip in the sideband heights for the fifth and tenth orders in the top trace are believed to be due to interference with the subfield stitching error of the machine because five subfields were used for these patterns.

Fig. 4 shows a close-up of the angular spectra for $M = 2$ and the same stitch error as in Fig. 2. The reduction in SMR is -25 dB. The notch in the suppressed side modes gives some indication of the shape of the filter. The reduction in SMR remained below -20 db even when varying the current dose by $\pm 30\%$. No special calibration of the dose was performed for the shot shifting. The dose was arrived at by dividing the dose for a standard grating by the number of passes used. This indicates that shot shifting is a robust process that may easily be incorporated into existing device patterns.

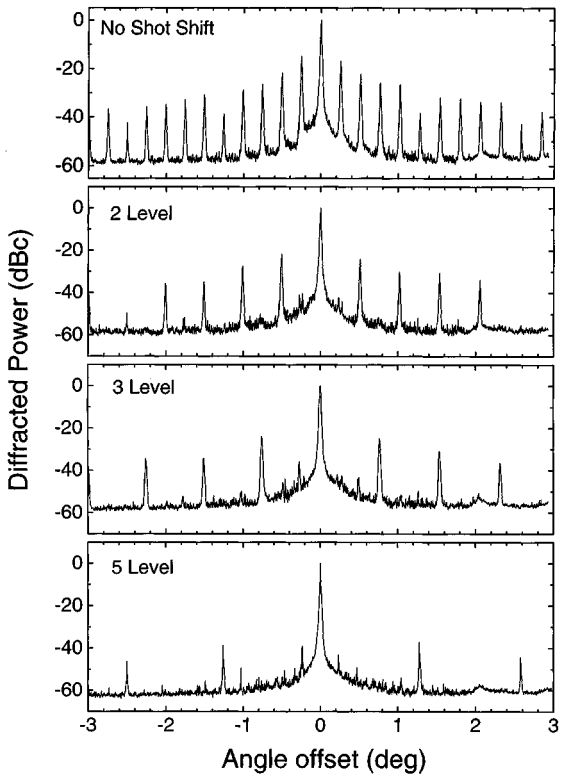

Fig. 3. Grating angular spectra for gratings with 26-nm intentional stitching error and different number of shot-shift levels.

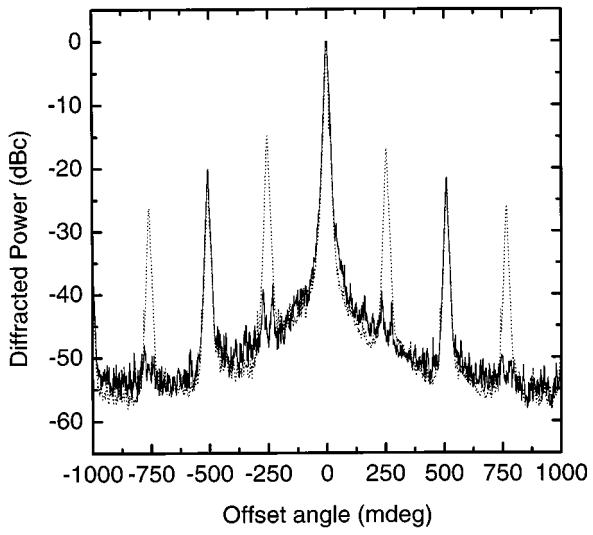

Fig. 4. Dotted curve: spectra with 26-nm stitching error. Solid curve: effect of two-level shot shifting yielding 25-dB reduction in the side-mode to main-mode ratio.

The diffraction measurements of Figs. 3 and 4 clearly show that the effect of M-order shot shifting is to suppress all $M-1$ nearest side modes. It is worth comparing shot shifting to a simple reduction in the field size, which would have the same effect of pushing the first significant side mode further away, where iy may not be harmful for a given application. For systematic errors, an M-fold reduction in the field size should translate to an equal reduction in the stitching error Δx, assuming it arises from sample bowing or tilt. As (1) and (2) show, stitching-error sidebands result from spectral components shifting of the zeros of $G_L(k)$, the single-field spectrum. The amplitude of the Mth sideband is the product of the slope of $G_L(k)$ at its Mth zero from the central peak, and the magnitude of the shift. The result is given by

$$G_{M,L} = \frac{N+M}{M}\frac{\Delta x}{L}. \tag{8}$$

This mode will slip through the filter $F_M(k)$ unaffected. Reducing the field size L by a factor of M, instead of shot shifting, will place the nearest side mode at the same detuning (it is now a first order side mode, however), but leave $\Delta x/L$ unchanged, so the magnitude will be

$$G_{1,L/M} = (N+1)\frac{\Delta x}{L}. \tag{9}$$

Surprisingly, the size of the first-order side mode is unaffected by reducing the field size (assuming a systematic Δx errors scale, as well). The ratio of these amplitudes shows that the magnitude of the nearest surviving side mode will be M times smaller for the shot-shifting case. Because the diffracted power can be expected to scale approximately as the square of the grating amplitude, this is a significant improvement in side-mode suppression ratio (SMSR). For random errors, because Δx should be independent of the field size in this case, even larger advantages can be expected.

IV. Stage Motion and Grating-Pitch Restrictions

Although higher orders of shot shifting suppress more of the nearest sidebands, it restricts the minimum accessible wavelength separation. The grating pattern is periodic in the stage-travel distance ΔL, which determines the grating spatial frequencies present by the delta comb in . (1). The minimum stage travel increment, therefore, determines the minimum shifts allowed in the grating k vectors. With no shot shifting, the minimum change in pitch is $\Delta L/N$. For M-order shot shifting, the end of the N/Mth grating period must lie on an allowed stage position. The minimum change in pitch allowed is then $\Delta LM/N$. The JEOL JBX-5D2 has a minimum stage increment of 10 nm. For $N = 200$ and $M = 5$, the minimum pitch separation is 0.25 nm. If this criterion is not satisfied, the zeros of the shot-shift filter, F_M in (7), will not lie exactly on the stitching-error sidebands, and the filtering will not be as effective. Situations requiring closely spaced pitches, such as matching DFB lasers to absorption lines and making distributed phase shifts in CPM lasers, will be limited in the number of shot-shift levels allowed. Note that abrupt phase shifts can be accommodated by using M special field patterns, with the phase shift at different positions in the field, and inserting them into the grating program at the desired location.

To show that the fundamental period of the grating is determined by the stage positioning, three gratings were written using five-level shot shifting and identical pitch (300 nm), but with different stitching errors of 0, 20, and 50 nm introduced by extra stage travel at the end of the field. The gratings were written 10 μm wide and placed adjacent to each other so that a single scan would capture diffraction of all three to accurately examine the relative peak positions. Fig. 5 shows the combined spectra with a

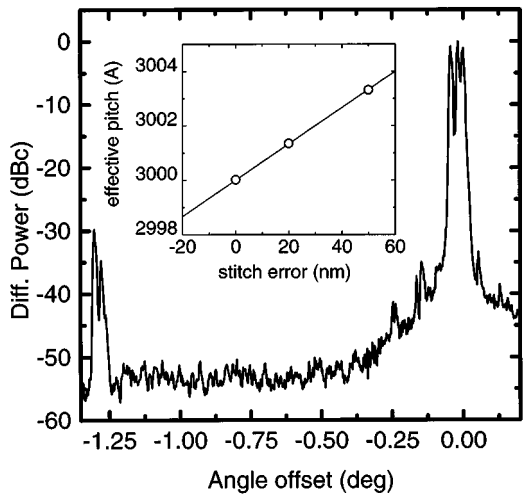

Fig. 5. Overlapping spectra of three gratings with identical (300 nm) pitch and 0-, 20-, and 50-nm stitching errors introduced by varying the stage travel. Insert: Circles show the effective pitches calculated from observed peak positions; solid line shows theory.

clearly evident shift of the peaks. The insert shows that the effective pitches calculated from the observed peak angles (circles) fall exactly as calculated (solid line). In this case, the pitch as written by the e-beam was fixed, and the stage travel increased. In practice, it is more common to desire small changes in the pitch while being forced to use the same field size. This result shows that changing the pitch size will have no effect, and the peak diffracted angle and spatial frequency will remain constant. In the grating with 20 nm of stitching error added, the shot shifting is not perfect because the stage must be moved in increments of $45\ \mu\text{m} + 4$ nm, which does not lie on the 10-nm stage position grid. This is the same effect as asking for pitches between the minimum separation $\Delta LM/N$, mentioned above. The observed sideband peaks remain -35 dB below the main peak despite the large stitching error, indicating that this limitation may not be so serious if the shot-shift notch filter is wide enough. Further experiments are underway to investigate this limit.

V. Conclusion

In conclusion, we have provided a simple linear model of the effect of multiple exposure techniques for reducing grating stitching error. The analysis demonstrates that M-level shot shifting will suppress the nearest $M - 1$ sidebands, and that increasing M will restrict the minimum separation in allowed pitches for a digitally controlled lithography machine. A robust 25-dB reduction in nearest sideband-diffraction efficiency was observed in optical diffraction measurements of gratings with intentional stitching error introduced. These results should help device designers to determine if shot shifting can be of benefit, and to develop appropriate multiple-write schemes for stitching-error reduction.

References

[1] T. Kjellberg and R. Schatz, "Investigation of the spectral characteristics of DFB lasers with different grating configurations made by electron-beam lithography," *J. Lightwave Technol.*, vol. 10, pp. 1256–1266, Sept. 1992.

[2] M. Okai, T. Tsuchiya, K. Uomi, N. Chinone, and T. Harada, "Corrugation-pitch modulated MQW-DFB lasers with narrow spectral linewidth," *J. Quantum Electron.*, vol. 27, pp. 1767–1772, June 1991.

[3] M. Suehiro, T. Hirata, M. Maeda, M. Hihata, and H. Hosomatsu, "GaAs/AlGaAs first-order gratings fabricated with electron beam lithography and very-narrow-linewidth long-cavity DBR laser diodes," *J. Quantum Electron.*, vol. 29, pp. 2081–2087, June 1993.

[4] Y. Muroya, T. Nakamura, H. Yamada, and T. Torikai, "Precise wavelength control for DFB laser diodes by novel corrugation delineation method," *Photonics Technol. Lett.*, vol. 9, pp. 288–290, Mar. 1997.

[5] J. Albert, S. Thériault, F. Bilodeau, D. C. Johnson, K. O. Hill, P. Sixt, and M. J. Rooks, "Minimization of phase errors in long fiber Bragg grating phase masks made using electron beam lithography," *Photonics Technol. Lett.*, vol. 8, pp. 1334–1336, Oct. 1996.

[6] R. C. Tiberio, D. W. Carr, M. J. Rooks, S. J. Mihailov, F. Bilodeau, J. Albert, D. Strykman, D. C. Johnson, K. O. Hill, A. W. McClelland, and B. J. Hughes, "Fabrication of electron beam generated, chirped, phase mask (1070.11–1070.66 nm) for fiber Bragg grating dispersion compensator," *J. Vac. Sci. Technol. B, Microelectron. Process. Phenom.*, vol. 16, pp. 3237–3240, 1998.

[7] J. Ye, C. N. Berglund, and R. F. W. Pease, "Spatial frequency filtering using multiple-pass printing," *J. Vac Sci. Technol. B, Microelectron. Process. Phenom.*, vol. 12, pp. 3455–3459, 1994.

David J. Dougherty received the B.S. degree inelectrical engineering from the University of Southern California, Los Angeles, in 1990 and the Ph.D. degree in physics from the Massachusetts Institute of Technology, Cambridge, in 1997 for research on ultrafast carrier dynamics in semiconductors.

At the Jet Propulsion Laboratory, California Institute of Technology, Pasadena, he has worked on grating design and fabrication for narrow-linewidth semiconductor lasers. Currently, he is developing grating-based integrated optical sensors for chemical and biological detection.

Richard E. Muller received the B.S. degree in chemical engineering from the University of Rochester, Rochester, NY, in 1984.

He joined the Jet Propulsion Laboratory, Center for Space Microelectronics, California Institute of Technology, Pasadena, in 1988. He is responsible for the operation of the JEOL JBX-5DII (JEOL USA, Peabody, MA 01960) electron-beam lithography system as well as the related sample processing.

Paul D. Maker received the Ph.D. degree in physics from the University of Michigan, Ann Arbor, in 1961.

He has worked in the fields of infrared molecular spectroscopy, lasers and nonlinear optics, hyper-Raman scattering, atmospheric chemistry, automotive emissions analysis studied by long-path Fourier transform infrared spectroscopy, and, most recently, electron-beam lithography and diffractive optics. Following a long career at the Ford Motor Company Scientific Research Laboratory, he joined the Jet Propulsion Laboratory, Center for Space Microelectronics Technology, California Institute of Technology, Pasadena, in 1987. There, he manages the electron-beam lithography lab as a Technical Group Leader. His current research centers upon innovative uses of the electron-beam machine, especially the fabrication of computer-generated e-beam fabricated holograms and other diffractive optic devices.

Siamak Forouhar received the Ph.D. degree in electrical engineering from the University of California, San Diego, in 1983. His dissertation was on fabrication and evaluation of diffraction grating lenses on $LiNbO_3$ waveguides.

He worked as a member of technical staff in the Fiber Optics Department, Collins Transmission Systems Division, Rockwell International, Dallas, TX, from 1983 to 1986 and Polaroid Corporation, Cambridge, MA, from 1986 to 1987. He joined the Jet Propulsion Laboratory, California Institute of Technology, Pasadena, in 1987 and became the Group Supervisor for Photonic Devices in 1992. His expertise is in the design and fabrication of photonic devices for spectroscopy and communication applications, especially the development of novel tunable laser-diode sources. He developed the world's first InGaAs strained-layer semiconductor laser in the 1.8–2.1 μm range.